investigations of areas that display these unusual scattering characteristics.

**References:** [1] Pettengill G. H. et al. (1991) *Science, 252,* 260–265. [2] Tyler G. L. et al. (1992) *JGR*, special Magellan issue, in press. [3] Ford P. G. (1992) *ARCDR Software Interface Specification* (CD-ROM USA_NASA_JPL_MG_2001). [4] Plaut J. J. et al., this volume.

**N93-14363**

## ANOMALOUS SCATTERING BEHAVIOR OF SELECTED IMPACT "PARABOLA" FEATURES: MAGELLAN CYCLE-TO-CYCLE COMPARISONS.

J. J. Plaut[1], R. S. Saunders[1], E. R. Stofan[1], R. L. Kirk[2], G. G. Schaber[2], L. A. Soderblom[2], P. G. Ford[3], G. H. Pettengill[3], D. B. Campbell[4], N. J. S. Stacy[4], R. E. Arvidson[5], and R. Greeley[6], [1]Jet Propulsion Laboratory, MS 230–225, 4800 Oak Grove Drive, Pasadena CA 91109, USA, [2]U. S. Geological Survey, Flagstaff AZ 86001, USA, [3]Center for Space Research, Massachusetts Institute of Technology, Cambridge MA 02139, USA, [4]National Astronomy and Ionospheric Center, Cornell University, Ithaca NY 14853, USA, [5]Department of Earth and Planetary Sciences, Washington University, St. Louis MO 63130, USA, [6]Department of Geology, Arizona State University, Tempe AZ 85287, USA.

**Introduction:** Magellan observations indicate that many venusian impact craters have associated surfaces, typically lower in backscatter and emissivity than the surroundings, that extend up to hundreds of kilometers to the west of craters, in parabolic planforms [1,2]. During Magellan's second mapping cycle, a number of these parabolic features were imaged for a second time, under a different viewing geometry. In some cases, the SAR backscatter appearance of portions of the parabolic features was quite different in the two datasets. In this paper, we present a description and preliminary interpretations of the anomalous appearance of these features as observed during Magellan's first and second mapping cycles.

**Observations:** Two types of structures within the parabolas show significant differences in appearance. These are "bright patches" and "streaks." Bright patches are irregular, diffuse-appearing areas of high backscatter (relative to surroundings). Values are typically 0 to 5 dB above the expected (Venus average) sigma zero, while surroundings are typically below the expected value. Differences in sigma zero between cycles can be as high as 9 dB, with comparable incidence angles but opposite look azimuths (cycle 1 east-looking, cycle 2 west-looking). Bright patches usually occur along the "arms" of the parabola features, but some are also seen in the central portions. Their distribution appears to be partly controlled by local small-scale (1–20 km) topography, such as wrinkle ridges. Discontinuous patches are often seen between (rather than straddling) wrinkle ridges, and some patches appear to terminate along ridges. Bright patch areas that are seen only in cycle 1 data occur at the craters Kuan Tao-sheng (–61.1, 181.7, 45 km), Eudocia (–59.1, 201.9, 29 km), and Boulanger (–26.5, 99.3, 57 km); patches seen only in cycle 2 data occur at the craters Stowe (–43.3, 233.2, 78 km), Kuan Tao-sheng, Austen (–25.0, 168.3, 47 km), Adaiah (–47.3, 253.3, 19 km), and Aksentyeva (–42.0, 271.9, 40 km).

"Streaks" are alternating high and low backscatter bands 1–20 km wide, up to 500 km long. The bright bands have still relatively low sigma zero values (within 2 dB of the expected), while the dark bands are almost always lower than the expected value. Streaks are often associated with, or are part of, bright patches. Trends of the streaks are consistently east-west, within about 10°. Like the bright patches, streaks are commonly truncated along wrinkle ridges. Streaks are more common near the axes of the parabolas (i.e., due west of the crater), although some also are seen on the parabola arms. At Kuan Tao-sheng and Eudocia, streaks seen in cycle 1 SAR data are rarely seen in cycle 2. At Stowe, many streak sets are visible only in cycle 2 data, some are visible only in cycle 1 data, while others are visible in both datasets.

Several areas that show anomalous scattering behavior in cycle 1 and cycle 2 SAR data also have unusual properties in the cycle 1 radiometry and altimetry-derived datasets. In particular, the Eudocia/Kuan Tao-sheng area, which shows an extensive (over 1500 × 2000 km) emissivity parabola, also displays extremely unusual behavior in the altimeter-derived reflectivity and rms slope parameters. The two parameters are highly correlated (high values in both) along a narrow hairpin-shaped parabolic feature approximately 800 × 2000 km in size. Many of the surfaces that show anomalously high cycle 1 SAR backscatter values (compared with cycle 2) occur on this hairpin-shaped feature. The magnitude of the rms slope (8°–10°) and reflectivity values (typically > 0.8; some >1.0) on otherwise smooth-appearing, moderately low emissivity plains, suggests that the altimeter echoes are not well-modeled by the Hagfors template matching procedure of [3]. Specifically, examination of the echo profiles shows that the anomalous areas have a wide dispersion in echo power with time. This accounts for the high rms slope solutions. The unphysical (>1.0) reflectivity values may result from a mismatch between the theoretical Hagfors quasispecular scattering formulation and the actual distribution of surface facets within the altimeter footprint.

To summarize the key observations: (1) The differences are only seen in association with impact crater parabola features. (2) The differences are seen in images taken with comparable incidence angles from opposite sides (at Kuan Tao-sheng/Eudocia, angles are within 5°, at Stowe within 3°). (3) The patterns of bright patched streaks are clearly associated with each other and with surface morphology (e.g., wrinkle ridges). (4) The most dramatic differences are confined to a single broad region of the planet: mid to high southern latitudes between Artemis and Phoebe. (5) The differences have both "senses," i.e., bright patches and streaks may be seen uniquely in either cycle 1 or cycle 2 data. (6) The Kuan Tao-sheng/Eudocia area shows anomalously high reflectivity and rms slope values in altimetry-derived data.

**Interpretations:** The first issue that must be addressed is this: Are the apparent differences in SAR backscatter between cycle 1 and cycle 2 data a result of a modification of the surface (or subsurface) during the eight-month interval between data acquisitions, or are they a result of an azimuthally biased surface (or subsurface) structure in which backscatter is strongly enhanced in either the east- or west-looking configuration?

The best test of the surface change hypothesis involves duplicating the geometry of the cycle 1 acquisition. This experiment, in the Stowe Crater region, should have been conducted by the time of this colloquium, and relevant results will be presented. cycle 1 and cycle 2 emissivity measurements, which were acquired at emission angles equivalent to the SAR incidence angles, show differences at the 2% level at Stowe and Kuan Tao-sheng, but the differences do not correlate well with the SAR differences. However, the bright patches and streaks do not have strong emissivity signatures in either cycle, so changes at the surface may not be detectable in emissivity. At present, altimetry-derived data from cycle 2 have not been reduced for these areas. The similar nadir-looking geometry of the cycle 1 and 2 altimetry measurements eliminates the look-

direction bias, and comparison of the reflectivity and rms slope parameters will also be presented at the colloquium.

The association of anomalous scattering behavior and impact parabola features suggests that impact-derived materials are involved. These probably have unique properties among Venus surface materials with respect to their size distribution (a large component of fines?) and possibly with respect to composition or mineralogy. The presence of streaks suggests that wind processes are involved. Under a surface change scenario, the variations in SAR backscatter are suggested to result from redistribution of a layer of loose material, possibly by wind, during the interval between data acquisitions. However, the scale of the observed differences requires large volumes of material to be redistributed over a short period of time. Furthermore, the common occurrence of impact parabola features on the planet indicates that the age of the population of parabolas is probably on the order of tens to hundreds of Ma. It seems unlikely, if these surfaces were vulnerable to such rapid change, that they would retain their distinctive signatures over such a time span.

The viewing geometry hypothesis requires surfaces that contain geometrical elements that favor or diminish backscatter strength, depending on the side from which the surface is observed. The very nearly identical incidence angles (though east- and west-looking), require that the surfaces have a strong asymmetrical component in the east-west direction. The dominant asymmetry in the parabolic features is in the east-west direction (parabolas "open" to the west), so it may be inferred that structures at a smaller scale have an east-west component of asymmetry. Aeolian bedforms (ripples, dunes) are the prime candidates for such structures in the parabola areas. Terrestrial transverse dunes typically have stoss slopes of 5°–10°, and slip face slopes of 30°–35°. The absence of the "speckly" returns commonly observed in SAR images of dunes implies that the bedforms responsible for the extensive bright patches contain faces at scales of tens of centimeters to no more than a few tens of meters. The visibility of aeolian bedforms in SAR imagery is known to be highly sensitive to look azimuth, relative to the dominant strike direction of slopes [4]. In the high southern latitudes discussed here, the look azimuth between cycles differed by ~160°, which may further affect the visibility of features. Several difficulties remain with the bedform hypothesis. The large enhancement in backscatter on steep faces should have a corresponding smaller enhancement on the shallow faces. This effect is not observed. The reversal in "sense" of the anomalies is also somewhat inconsistent with bedforms developed within a wind regime dominated by one persistent direction of flow, necessary for such widespread, consistent slope distributions.

**References:** [1] Arvidson R. E. et al. (1991) *Science, 252,* 270–275. [2] Campbell D. B. et al. (1992) *JGR,* special Magellan issue, in press. [3] Pettengill G. H. et al. (1991) *Science, 252,* 260–265. [4] Blom R. G. (1988) *Int. J. Rem. Sens., 9,* 945–965.

# N93-14364

## CYTHEREAN CRUSTAL BENDING AT SALME DORSA.

J. Raitala and K. Kauhanen, Department of Astronomy, University of Oulu, Finland.

The horseshoe-like, narrow (100 km wide and 600 km long) Salme Dorsa consists of arcuate ridges and grooves opening southeast on the planitia to the south of Ishtar Terra. Magellan radar data was studied in order to find tectonic style and lithospheric thickness of the area. The Salme ridge belt indicates folding and thrust faulting of surface layers due to compression against the tessera foreland zone. The western edge of Salme Dorsa is scarplike. Most ridges follow the main course of the arc and the overall ridge orientation is north-south while ridges subparallel the arcuate edge. The ridge trend at the northeastern end is northeast-southwest, while the southern part of the horseshoe has more northwestern ridges. The ridge belt has elements of normal compression against the zone. It has widened due to the new ridge formation. As this process repeats itself, the crust also becomes thicker making the topographically high ridge belt act as a load.

The scarp along the western edge of Salme Dorsa indicates that the movement has been to the west or northwest. West of Salme Dorsa the crust has bent due to the load and/or thrust of Salme Dorsa, resulting in a trough outside the scarp. The compressional ridge belt has acted either as a nappe overthrust or as a mere surface load due

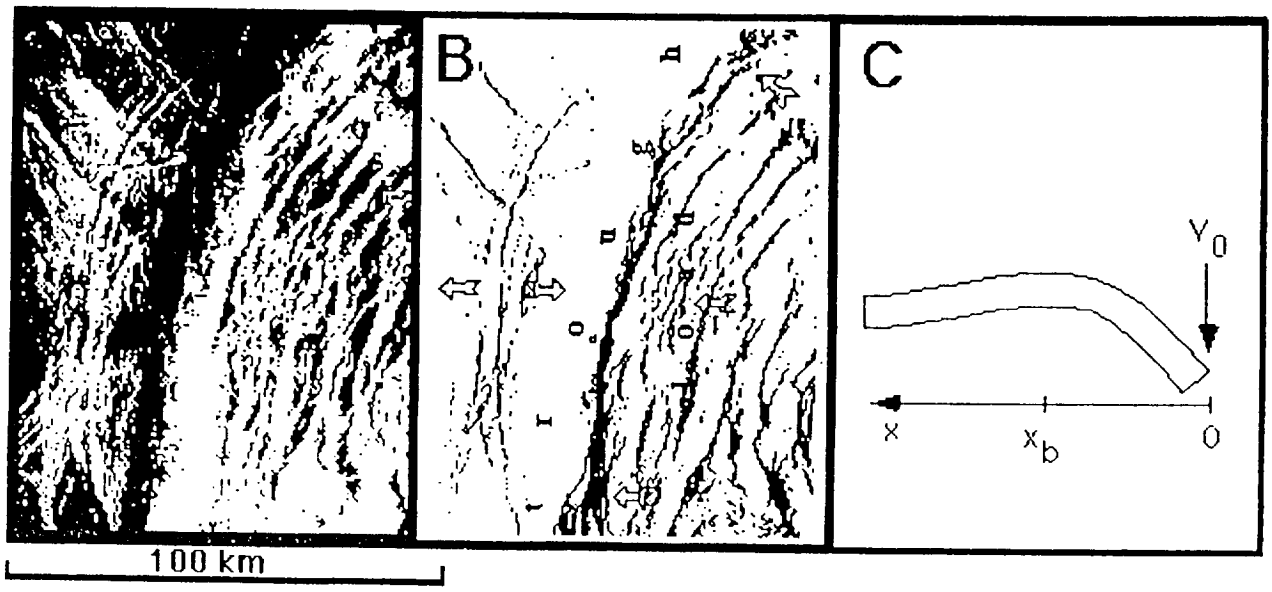


Fig. 1. Radar image of the crustal bending at central Salme Dorsa (a). The load and compression/tension stress system is displayed (b) and modeled with vertical exaggeration (c). The trough depression is next to a surface load and/or compressional massif. Grabens are located on the anticlinal bulge.